

This article was downloaded by:

On: 24 January 2011

Access details: *Access Details: Free Access*

Publisher *Taylor & Francis*

Informa Ltd Registered in England and Wales Registered Number: 1072954 Registered office: Mortimer House, 37-41 Mortimer Street, London W1T 3JH, UK



## Journal of Macromolecular Science, Part A

Publication details, including instructions for authors and subscription information:

<http://www.informaworld.com/smpp/title~content=t713597274>

### Analysis of the Pore Structure of Ion-Exchange Resins and the Adsorption Equilibrium of $\text{Fe}^3/\text{Cl}^-$ Complex Ions

Kunihiko Takeda<sup>a</sup>; Fumiaki Kawakami<sup>a</sup>; Mitsunaga Sasaki<sup>a</sup>

<sup>a</sup> Research & Development Division Asahi Chemical Industry Co., Ltd, Kawasaki, Japan

**To cite this Article** Takeda, Kunihiko , Kawakami, Fumiaki and Sasaki, Mitsunaga(1986) 'Analysis of the Pore Structure of Ion-Exchange Resins and the Adsorption Equilibrium of  $\text{Fe}^3/\text{Cl}^-$  Complex Ions', Journal of Macromolecular Science, Part A, 23: 9, 1137 – 1154

**To link to this Article:** DOI: 10.1080/00222338608081119

**URL:** <http://dx.doi.org/10.1080/00222338608081119>

PLEASE SCROLL DOWN FOR ARTICLE

Full terms and conditions of use: <http://www.informaworld.com/terms-and-conditions-of-access.pdf>

This article may be used for research, teaching and private study purposes. Any substantial or systematic reproduction, re-distribution, re-selling, loan or sub-licensing, systematic supply or distribution in any form to anyone is expressly forbidden.

The publisher does not give any warranty express or implied or make any representation that the contents will be complete or accurate or up to date. The accuracy of any instructions, formulae and drug doses should be independently verified with primary sources. The publisher shall not be liable for any loss, actions, claims, proceedings, demand or costs or damages whatsoever or howsoever caused arising directly or indirectly in connection with or arising out of the use of this material.

## **Analysis of the Pore Structure of Ion-Exchange Resins and the Adsorption Equilibrium of $\text{Fe}^{3+}/\text{Cl}^-$ Complex Ions**

KUNIHICO TAKEDA, FUMIAKI KAWAKAMI, and  
MITSUNAGA SASAKI

Research & Development Division  
Asahi Chemical Industry Co., Ltd.  
1-3-2 Yako, Kawasaki-ku, Kawasaki 210, Japan

### **ABSTRACT**

The microstructure of ion-exchange resins has been investigated to understand more clearly the ion-exchange mechanism. Nine types of resins with different pore structures were used: all of the polystyrene family crosslinked with divinylbenzene and anionic resins, with mesh sizes ranging from 100 to 200, except for one (20-50 mesh). Various pore volumes of each resin were determined by measurements of intrusion of some chemical species ( $\text{H}_2\text{O}$ ,  $\text{Nd}^{3+}$ , and  $\text{Hg}$ ) into the resin. The results are analyzed on the basis that an ion-exchange resin particle consists of four regions. They are: 1) the mercury intrusion region, 2) the region where coions (such as  $\text{Nd}^{3+}$ ) can intrude but mercury cannot, 3) the region where water or counterions can intrude but coions cannot, and 4) the polymer matrix region occupied by the polymer skeleton. The former two regions are not influenced by the resin-fixed ionic groups. While it used to be thought that specific adsorption of counterions may occur in the entire exchange resin particle, it is appropriate to consider that specific adsorption

takes place only in the latter two regions. According to this point of view, the adsorption equilibrium of the  $\text{Fe}^{3+}/\text{Cl}^-$  complex ions could be explained more satisfactorily.

## INTRODUCTION

Empirical and theoretical analyses of the equilibrium behavior of ions in ion-exchange resins have been studied based on the assumption that the interior of an ion-exchange resin is a homogeneous electrolyte solution [1]. Most studies of ion exchange describe the equilibrium behavior of ions, mainly of counterions with the charge sign opposite to the resin-fixed charge. A theoretical approach for the exclusion of coions with the same charge sign as the fixed ions from an ion-exchange resin was originally established by Donnan [2, 3]. The exclusion is strongly dependent on the concentration of fixed ionic groups.

According to the above "homogeneous" assumption, the entire particle of the ion-exchange resin is taken as the adsorption phase, and a hypothetical Donnan membrane is set up at the resin-particle surface. However, it has often been observed that coions other than those of the Donnan salt are contained even in gel-type ion-exchange resins, and it is apparent that macroporous ion-exchange resins can extensively accommodate coions in their macropores.

In order to clarify ion-exchange behavior more clearly, we have focused on close analysis of the microstructure of ion-exchange resins. A macroporous ion-exchange resin may be one of the most interesting materials for this purpose because the pore structure can be directly observed by electron microscope and other methods. Macroporous ion-exchange resin have been prepared since 1960 with the aim of improving the performance in practical applications [4]. There are, however, few studies which relate the ion-exchange characteristics of ion-exchange resins to their physical fine structures [5].

Such information is required for the molecular design of ion-exchange resins with appropriate properties. The different selectivity coefficients have often been reported in ion-exchange studies, and this limits the elucidation of ion-exchange behavior because of the lack of physical and chemical characteristics of the ion-exchange resins, such as the location of the Donnan membrane. The purpose of this study is to analyze the pore structure of ion-exchange resins and to clarify its relation to ion-exchange behavior. Then the applicability of the results to the ion-exchange equilibrium of  $\text{Fe}^{3+}/\text{Cl}^-$  complex ions will be examined.

## EXPERIMENTAL

Ion-Exchange Resins

Nine types of anion exchange resins were used. Three were commercially available, and the other six were prepared in our laboratory. The experimental resins, GR-1 to GR-6, were prepared principally according to the conventional method by suspension polymerization. The general protocol for resin synthesis begins with polymerizing a mixed monomer solution of chloromethylstyrene (a mixture of *m*- and *p*-isomers, 80 parts) and *m*-divinylbenzene (20 parts). The mixed monomers are suspension polymerized with 1 part of azobisisobutyronitrile as initiator in aqueous medium. Then the spherical resin obtained is reacted with an excess of trimethylamine. The resulting resins are strongly anionic, and their fixed ionic groups are tetraalkylammonium cations. Of the commercially available anion-exchange resins, Dowex 1-X8 is a tetraalkylammonium type, Dowex 2-X8 is a hydroxylated tetraalkylammonium type, and Dowex 11 is a more porous resin than Dowex 1-X8, though with essentially the same chemical composition as 1-X8. The properties of all the resins are listed in Table 1.

Measurements of Ion-Exchange Capacity

The ion-exchange capacity was measured according to the conventional method at 25°C by the use of a jacketed Pyrex column 1 cm in diameter and 20 cm long.

The ion-exchange behavior of complex ions was measured with the same apparatus as used for the measurements of the ion-exchange capacity. After ion-exchange equilibrium was attained, the adsorbed ions were eluted and their quantities were measured by spectrophotometry.

Measurements of Pore Volumes

The pore volumes of ion-exchange resins were measured according to the following three methods:

- 1) The method based on water content and density of resin
- 2) The pressurized-mercury intrusion method
- 3) The nonexchangable ion pulse method

TABLE 1. Properties of Ion-Exchange Resins

	CL <sup>a</sup>	IEC, <sup>b</sup> mol/kg	d <sub>s</sub> , <sup>c</sup> kg/L	f <sub>t</sub> <sup>d</sup>	f <sub>f</sub> <sup>e</sup>
Dowex 1x8	8	3.5	1.10	0.43	0.01
Dowex 2x8	8	3.5	1.13	0.41	0.01
Dowex 11	-	4.0	1.12	0.53	0.01
GR-1	16	2.8	1.14	0.61	0.40
GR-2	16	2.8	1.14	0.61	0.27
GR-3	16	2.8	1.14	0.61	0.01
GR-4	16	2.1	1.10	0.59	0.38
GR-5	16	2.1	1.10	0.59	0.25
GR-6	16	2.1	1.10	0.59	0.01

<sup>a</sup>Crosslinking (wt% DVB).

<sup>b</sup>Ion-exchange capacity (dry resin).

<sup>c</sup>Density.

<sup>d</sup>Total pore ratio.

<sup>f</sup>Fixed pore ratio.

The pore volume, which is determined by the method based on the water content/density, is defined as the total pore volume, because water may intrude so deeply as to contact throughout the resin matrix.

In the pressurized-mercury intrusion method, a mercury porosimeter (Carlo/Elba 200 size) was used. Two types of void are detected by this method: one is the inherent pores within the resin particles and the other is the interstices between the packed resin particles. The inherent pores can be distinguished from the interstices by their pore sizes. The interstices show pore sizes larger than a few  $\mu\text{m}$ , i.e., larger by about one order of magnitude than the largest inherent pores within resin particles. It is instructive to trace the curves shown in Fig. 1. Both types of resins have sharp peaks at a small pore size range. Well beyond this peak, one finds the foot of another peak around 2 000 nm.

From these examples, the pores less than 800 nm in diameter are properly regarded to be inherent pores inside the particles, whereas the pores of more than 2 000 nm can be considered to be the packing interstices between the resin particles. In effect, pores of 5 to 800 nm in diameter are assigned to be inherent within particles, and they are called "fixed pores."

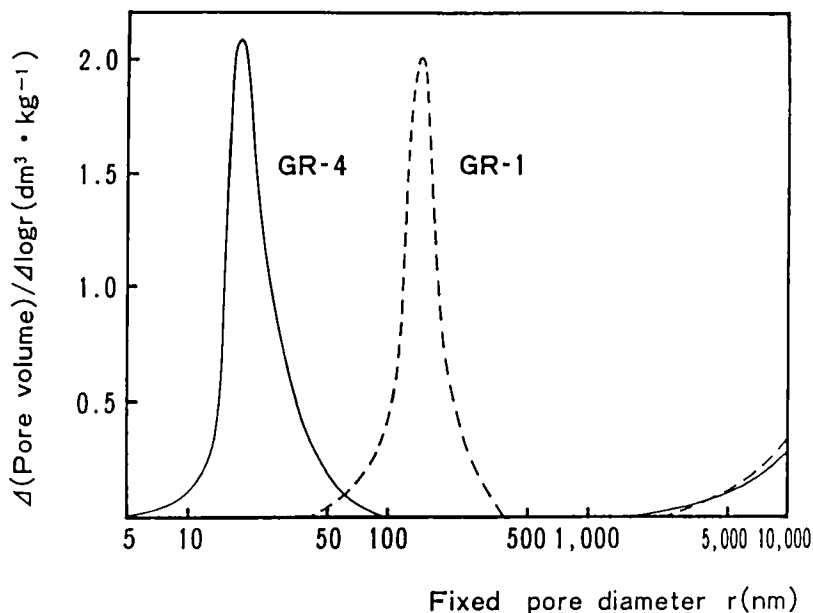


FIG. 1. Pore size distribution of ion-exchange resins by the pressurized mercury intrusion method.

The pore volume, which is measured by the nonexchangeable ion pulse method, is assigned to the region where coions intrude. A jacketed Pyrex column (1 cm inner diameter and 50 cm long) was packed with ion-exchange particles. After conversion to the  $\text{Cl}^-$  form, a tracer-level amount of 1 M solution of  $\text{NdCl}_3$  dissolved in 1 N HCl was injected into the column. The retention volume of  $\text{Nd}^{3+}$  ions was measured at 795 nm using a spectrophotometric detector equipped with a flow cell. The outer void fraction is defined as the ratio of the total void volume outside the packed particles to the bed volume. It was calculated from the total pore volume, the weight and specific gravity of the ion-exchange resin, and the bed volume. From the retention volume  $V_R$ , the outer void fraction  $\epsilon_0$ , and the bed volume  $V_0$ , the volume of the coion intrusion region is obtained. The ratio of the above volume to the total resin volume, which is defined as the coion pore ratio  $f_i$ , can be calculated as follows:

$$f_i = \frac{V_R - V_0 \epsilon_0}{V_0 (1 - \epsilon_0)} \quad (1)$$

Lanthanide ions, such as  $\text{Nd}^{3+}$ , are known to be nonexchangeable on an anion-exchange resin even in 12 M HCl solution [6, 7].  $\text{Nd}^{3+}$  ions remain positively charged in these chloride solutions, and thus  $\text{Nd}^{3+}$  is suitable as a probe for searching the region where nonexchangeable ions intrude.

## RESULTS AND DISCUSSION

### The Four Regions of an Ion-Exchange Resin

Table 1 shows ion-exchange capacities, densities, total pore ratios  $f_t$ , and fixed pore ratios  $f_f$ . The total pore ratio was found to be in the range of 0.41-0.53 for the Dowex ion exchangers, while it was approximately 0.6 for all the synthesized ion-exchange resins. The fixed pore ratios of GR-3, GR-6, and Dowexes are relatively low as 0.01, while they are 0.25-0.4 in GR-1, GR-2, GR-4, and GR-5.

Table 2 shows the coion pore ratios  $f_i$  measured according to the nonadsorbable ion pulse method. The outer void fraction  $\epsilon_0$  was found to be nearly constant for all the resins. The coion pore ratios of GR-3 and GR-6 are 0.25 and 0.28, respectively, and those of GR-1, GR-2, GR-4, and GR-5 are as high as 0.45-0.54, while those of Dowexes are 0.19-0.24. These values indicate that GR-1, GR-2, GR-4, and GR-5 have higher fixed pore ratios to permit intrusion of coions.

Figure 1 shows the pore size distribution curves for GR-1 and GR-4, measured with the mercury porosimeter. The fixed-pore size is centered at 100 nm, ranging from 40 to 300 nm, in GR-1, and at 20 nm, ranging from 10 to 100 nm, in GR-4. Figure 2 shows electron micrographs of cross sections of particles of GR-1 and GR-3. The pore structure of GR-1 can be seen to be clearly distinguished from the resin matrix, while the cross section of a GR-3 particle is apparently homogeneous. As described above, the present measurements can discriminate the following three pore regions:

- 1) Total pore region: the region where water intrudes
- 2) Fixed pore region: the region with pore diameters between 5 and 800 nm where mercury can be intruded under pressure
- 3) Coion pore region: the region where nonexchangeable ions can migrate.

The volumes of these pore regions decrease in the order, total pore region > coion pore region > fixed pore region, as shown in Tables 1 and 2. On account of the measurement conditions of these pore volumes, there may be some overlap among these regions. To make clear the relationship among the three regions, it is assumed that a

TABLE 2. Measurement of Coion Pore Ratios by the Column Method

	$\epsilon_0^a$	$V_R^b$	$f_i^c$
Dowex 1x8	0.41	20.4	0.19
Dowex 2x8	0.42	20.4	0.20
Dowex 11	0.41	21.6	0.24
GR-1	0.41	28.7	0.53
GR-2	0.41	26.7	0.45
GR-3	0.42	22.4	0.25
GR-4	0.41	28.7	0.54
GR-5	0.41	26.3	0.45
GR-6	0.42	22.8	0.28

<sup>a</sup>Outer void fraction.

<sup>b</sup>Retention volume.

<sup>c</sup>Coion pore ratio.

resin particle may be divided into four regions, A, B, C, and D, as shown schematically in Fig. 3. The cross-hatched Region A represents the polymer matrix region, and Region D refers to the fixed-pore region. Foreign substance enters into the particle from the surface at the right. Both water and counterions intrude as far as Region B. Coions like  $Nd^{3+}$  enter into Region C through Region D, and mercury enters into Region D but not further. Thus, the total pore region consists of B, C, and D, and the hypothetical Donnan membrane is located as the boundary between Regions B and C.

In the present treatment, an ion-exchange resin particle can be considered to consist of polymer matrix and total pores, that is,

$$f_t + f_p = 1, \tag{2}$$

where  $f_p$  is the volume fraction of polymer matrix and  $f_t$  is the volume fraction of total pores.

Table 3 summarizes the results of volume fraction determination. Figure 4 shows the volume fractions of the four regions in GR-1, GR-2, and GR-3, whose total pore ratios are equal to each other. These three types of ion-exchange resins differ greatly in the volume fractions of Regions B and D.



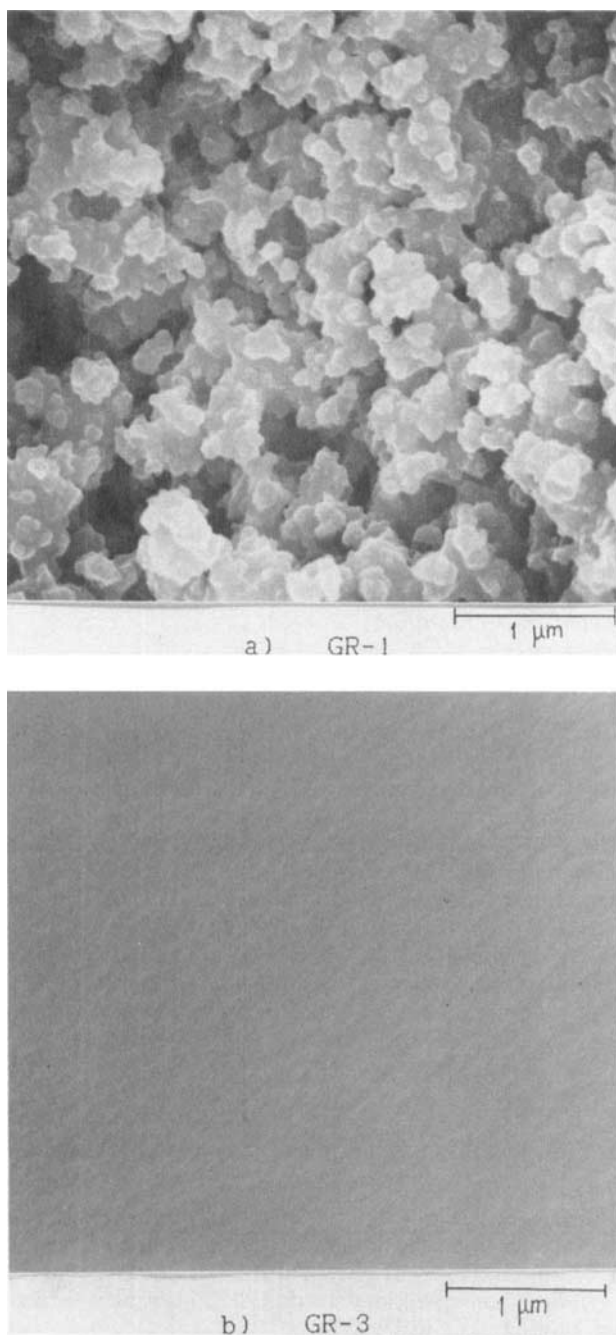


**FIG. 2.** Electron micrographs of the cross sections of ion-exchange resin particles.

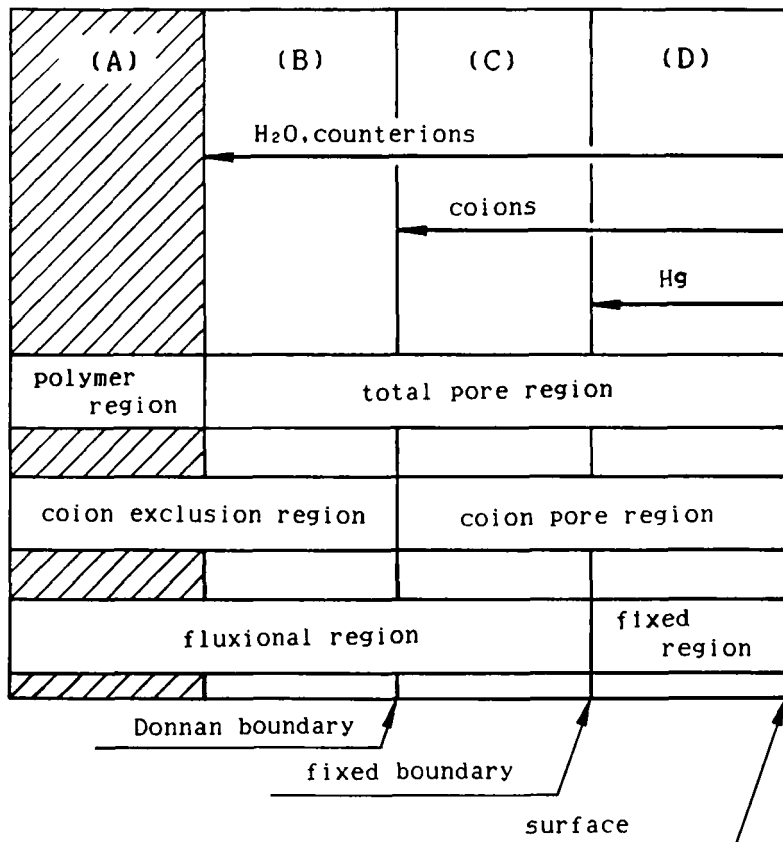


FIG. 3. Schematic model for the structure of an ion-exchange resin particle.

By taking these resins as examples, the four regions of ion-exchange particles could be characterized as follows:

Region A is the exclusive volume of polymer chains and fixed ionic groups.

Region B is considered to be under the Donnan effect resulting from the strong electrostatic field of the fixed ionic groups. This is certainly the region where the exchange of counterions takes place. The volume fraction of this region is given by  $(f_t - f_i)$ ; 0.08, 0.16, and 0.36 for GR-1, GR-2, and GR-3, respectively; it varies inversely with the fixed pore ratio.

TABLE 3. Volume Fractions<sup>a</sup> of the Four Regions of the Ion-Exchange Resins

	$f_t^b$	$f_p^c$	$f_f^d$	$(f_t - f_f)^e$	$f_i^f$	$f_x^g$
Dowex 1x8	0.43	0.57	0.01	0.42	0.19	0.81
Dowex 2x8	0.41	0.59	0.01	0.40	0.20	0.80
Dowex 11	0.53	0.47	0.01	0.52	0.24	0.76
GR-1	0.61	0.39	0.40	0.21	0.53	0.47
GR-2	0.61	0.39	0.27	0.34	0.45	0.55
GR-3	0.61	0.39	0.01	0.60	0.25	0.75
GR-4	0.59	0.41	0.38	0.21	0.54	0.46
GR-5	0.59	0.41	0.25	0.24	0.45	0.55
GR-6	0.59	0.41	0.01	0.59	0.28	0.72

<sup>a</sup>Volume fraction is defined as the ratio of each volume to the whole volume.

<sup>b</sup>Total pore ratio.

<sup>c</sup>Polymer matrix ratio.

<sup>d</sup>Fixed pore ratio.

<sup>e</sup>Fluxional pore ratio.

<sup>f</sup>Coion pore ratio.

<sup>g</sup>Volume fraction of coion exclusion region, equal to  $(1 - f_i)$ .

The volume fraction of Region C is given by  $(f_i - f_f)$ ; 0.13, 0.18, and 0.24 for GR-1, GR-2, and GR-3, respectively. This region consists of the pores smaller than 5 nm in diameter, into which coions can intrude. The pore size of 5 nm is critical in considering the physico-chemical properties of the ion-exchange resins. In our measurement of pore sizes of 3.7–5 nm with the mercury porosimeter under high pressure, each run gave a different nonreproducible value. We also attempted to measure the surface area of an ion-exchange resin with a high proportion of pores smaller than 5 nm by the low-temperature nitrogen adsorption method (BET method), but accurate data could not be obtained. These results suggest that the pores smaller than 5 nm may not be present in a fixed state but fluctuate. This region is formed as interstices between polymer chains with thermal motion. This region decreases significantly with increasing fixed pore volume, as shown in Fig. 4. It is suggested that polymerization under higher spatial restrictions gives more rigid polymer chains, which yield a larger fixed-pore volume.

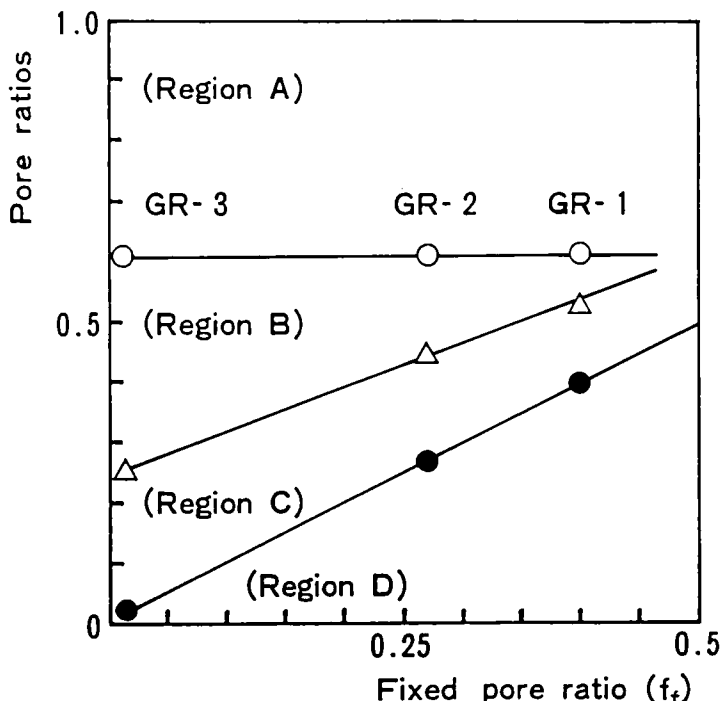


FIG. 4. Pore ratios  $f_t$  ( $\circ$ ),  $f_i$  ( $\Delta$ ), and  $f_f$  ( $\bullet$ ) in relation to fixed pore ratio for GR-1, GR-2, and GR-3.

Region D consists of pores clearly distinguishable from the resin skeleton, as can be seen in the electron micrograph of a GR-1 particle (Fig. 2). The volume fraction  $f_f$  is 0.40, 0.27, and 0.01 for GR-1, GR-2, and GR-3, respectively. This region is occupied by a solution of the same composition as the external solution in which the resin is immersed.

Of the three pore regions, Region D is rigidly fixed, while Regions B and C may fluctuate in position. These regions are considered to be at least partially exchangeable in spatial position because thermal motion of the polymer chains prevails in these regions.

The comparison of GR-4, GR-5, and GR-6, another series of resins with the same total pore ratio and the same exchange capacity, gave results similar to those shown in Fig. 4 for the series GR-1, GR-2, and GR-3.

TABLE 4. Concentrations of  $\text{Fe}^{3+}$  Ions Adsorbed in Ion-Exchange Resins

	$C_{\text{Cl}^-}$ , <sup>a</sup> mol/L	$C_{\text{Fe}^{3+}}$ , <sup>b</sup> mol/L	$C_{\text{Fe},r}$ , <sup>c</sup>	
			(a), <sup>d</sup> mol/L	(b), <sup>e</sup> mol/L
GR-1	5	0.022	0.49	0.24
		0.098	1.46	0.74
		0.201	2.07	1.08
		0.297	2.40	1.28
GR-2	5	0.022	0.55	0.31
		0.098	1.46	0.85
		0.201	1.98	1.18
		0.297	2.24	1.37
GR-3	5	0.022	0.71	0.54
		0.098	1.43	1.10
		0.201	1.75	1.36
		0.297	1.90	1.50

<sup>a</sup>Concentration of  $\text{Cl}^-$  ions in solution.

<sup>b</sup>Concentration of  $\text{Fe}^{3+}$  ions in solution.

<sup>c</sup>Concentration of  $\text{Fe}^{3+}$  ions adsorbed on an ion-exchange resin.

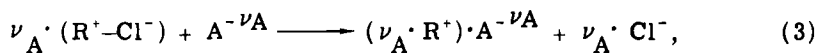
<sup>d</sup>Concentration based on the summed volume of Regions A and B.

<sup>e</sup>Concentration based on the whole particle volume.

### Coion Exclusion Region and Complex Ion Adsorption Equilibria

Table 4 shows results for the ion-exchange equilibrium of the complex ion  $\text{Fe}^{3+}/\text{Cl}^-$  on GR-1, GR-2, and GR-3. These ion-exchange resins have essentially the same ion-exchange capacity and total pore ratio. The solutions had constant  $\text{Cl}^-$  ion concentration, but that of  $\text{Fe}^{3+}$  was varied. The ionic strength of the solutions was approximately constant at 5.0 because it is determined principally by the concentration of  $\text{Cl}^-$  ions.

The exchange reaction of complex ions on an anion-exchange resin can be expressed by



where  $R^+$  represents a fixed ionic group and  $A^{-\nu_A}$  is a complex ion with a negative charge of  $\nu_A$ .

The total adsorption capacity  $C_t$  of an ion-exchange resin is the sum of the fixed ionic group concentration and the Donnan salt concentration. Thus,

$$C_t = \frac{\sqrt{C_R^2 + 4C_A \cdot C_{Cl}} + C_R}{2}, \quad (4)$$

where  $C_R$  is the concentration of fixed ionic groups (ion-exchange capacity), while  $C_A$  and  $C_{Cl}$  are the concentrations of ion  $A^{-\nu_A}$  and  $Cl^-$  ion, respectively, in the solution.

Equations (3) and (4) lead to

$$K_{Cl}^A = \left( \frac{C_{A,r}}{C_A} \right) \left/ \left\{ \frac{(\sqrt{C_R^2 + 4C_A \cdot C_{Cl}} + C_R) - 2\nu_A \cdot C_A}{2C_{Cl}} \right\}^{\nu_A} \right., \quad (5)$$

where  $K_{Cl}^A$  is the molar selectivity coefficient in Eq. (3) and  $C_{A,r}$  is the concentration of the adsorbed ion  $A^{-\nu_A}$ .

If  $K_{Cl}^A$  and  $\nu_A$  are constant in a certain range of ion concentrations, plots of  $K_{Cl}^A$  against  $\nu_A$  for the various concentrations of ions should all intersect at a single point on the  $\nu$ -K plane. Examples are shown in Fig. 5, where four curves correspond to four experimental data. The values of  $\nu_A$  at this intersection indicates the average valence number of the complex ions adsorbed by the ion-exchange resin [8].

In order to determine the adsorption phase concentrations, it is required that a boundary between the adsorption phase and the solution phase be determined. Here the adsorption phase is assumed according to the following two approaches: (a) based on the hypothesis that the ion-exchange equilibrium holds across a hypothetical Donnan membrane between the coion exclusion region and the coion pore region; and (b) based on the conventional hypothesis that the equilibrium takes place across the surface membrane between the exchanger par-

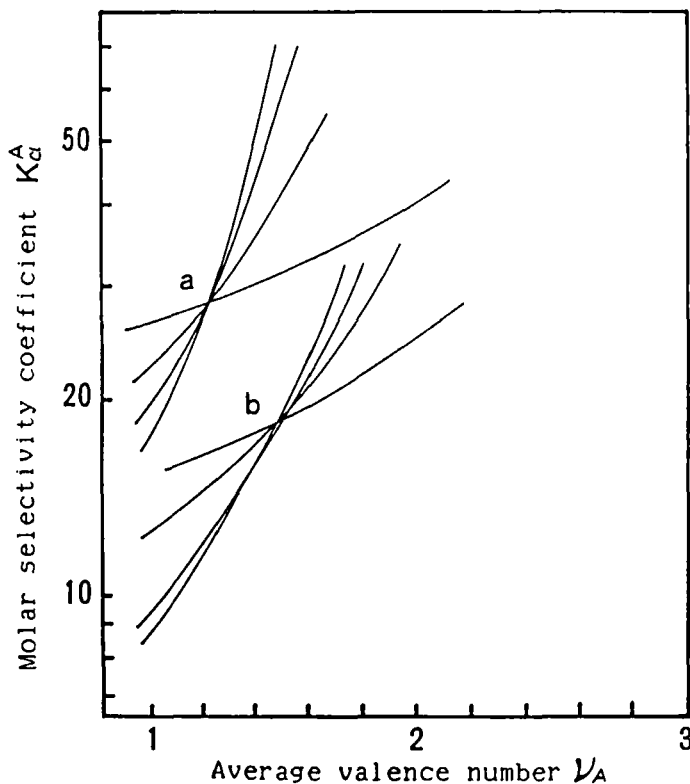


FIG. 5.  $\nu_A - K_{Cl}^A$  curves of the GR-1 exchange resin. (a) Based on coion exclusion region. (b) Based on the whole particle.

ticle and the external solution, i.e., the particle surface is regarded as a hypothetical Donnan membrane.

In Approach (a), the ion-exchange of the  $Fe^{3+}/Cl^-$  complex ions is considered to take place only in the coion exclusion region. Here it was assumed that the concentration of  $Fe^{3+}$  ions in coion pores is the same as in the external solution. In Approach (b) the ion-exchange resin as a whole is regarded as a homogeneous adsorption phase, and  $Fe^{3+}$  ions in pores are counted as the adsorbed ions.

The  $\nu$ -K plots of Eq. (5) for GR-1 based on both approaches are shown in Fig. 5. For Approach (a), the curves intersect exactly at one point,  $\nu = 1.2$ ,  $K = 28.3$ . The coincidence at one point is also observed for other GR resins. In contrast, for Approach (b), the intersections do not converge to one point in the  $\nu$ -K plane (Fig. 5). It can be concluded from these results that a uniquely defined ion-ex-

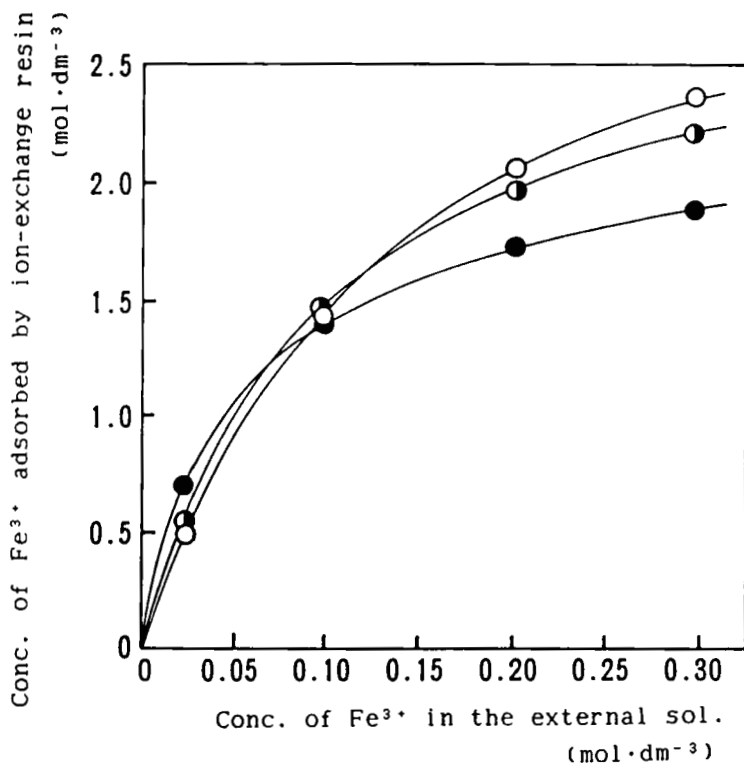


FIG. 6. Adsorption isotherms (solid lines) of Fe<sup>3+</sup>-Cl<sup>-</sup> complexes. Experimental values for GR-1 (○), GR-2 (◐), and GR-3 (●).

change constant is derived from the proposition that the coion exclusion region is an adsorption phase and the concentration of ions in the coion pore region is the same as in the external solution. The theoretical adsorption isotherms calculated by using  $\nu$  and  $K$  values based on the coion exclusion region approach give good agreement with the measured values even in a range of high concentrations, as shown in Fig. 6.

The selectivity coefficient  $K$  is one of the most fundamental and important indexes for studying ion-exchange equilibrium. In all the studies reported hitherto, the selectivity coefficients have been measured by Approach (b). Thus, these values do not correctly depend on the concentrations of ions influenced by the fixed ionic groups but on the arbitrarily averaged concentrations of ions influenced by the fixed ionic groups and ions in the solution. In this study the selec-



tivity coefficients for GR-4, GR-5, and GR-6 were estimated to be 28.2, 34.5, and 70.8, respectively, by Approach (a).

The  $\nu$  values falling in a range of 1.2-1.6 (for GR-1, GR-2, and GR-3) indicate that complex ions  $\text{FeCl}_4^-$  and  $\text{FeCl}_5^{2-}$  coexist within the ion-exchange resin as exchangeable ions. The volume fraction of the coion exclusion region to the whole volume of particles is expressed as  $f_x$  (Table 3).

The difference in  $\nu$  (1.2 in GR-1 with  $f_x = 0.47$  and 1.6 in GR-3 with  $f_x = 0.75$ ) supports the above discussion that GR-3 has a higher freedom of polymer motion than GR-1. The higher flexibility of the polymer chains favors the adsorption of polyvalent complex anions having inherently higher adsorption ability.

There are some literature reports that only one species of complex ions is adsorbed on the ion-exchange resin, as suggested by the reflectance spectra of the resin-bound complex ions [9], the stoichiometric methods [10, 11], and the method based on the distribution coefficient [12]. However, our observed nonintegral valences of the  $\text{Fe}^{3+}/\text{Cl}^-$  complexes, together with the theoretical consideration in this study, suggest that several species of complexes simultaneously exist on the ion-exchange resin. The distribution of the complexes on the ion-exchange resin are now being studied in detail and will be the subject of forthcoming reports.

## CONCLUSIONS

(1) It was assumed that four regions comprise a particle of ion-exchange resin: 1) the polymer matrix Region A, 2) Region B where counterions can intrude but coions cannot, 3) Region C where coions can intrude but mercury cannot, and 4) the mercury intrusion Region D.

(2) It was found that the ion-exchange behavior can be uniquely described based on the proposition that the former two (coion exclusion region) are taken as the adsorption phase, and the latter two (coion pore region) as the solution phase. This treatment gave a better graphical solution of the equation for the complex ion-exchange equilibrium than the old treatment, which regards the whole particle as the adsorption phase. This result suggests that a hypothetical Donnan membrane should be located within ion-exchange particles.

(3) The adequacy of this treatment was supported by good agreement between the calculated and experimental adsorption isotherms for  $\text{Fe}^{3+}/\text{Cl}^-$  complex ions.

(4) The estimated values of valence number  $\nu$  of exchanged complex ions were not integral. This suggests that more than one species of complex ions is exchangeable on the ion-exchange resins.

## ACKNOWLEDGMENTS

We are greatly indebted to Professor T. Tsuruta of the Science University of Tokyo and Professor M. Seno of Tokyo University for a number of useful instructions and advice received in performing the present study.

## SYMBOLS

$C_A$	concentration of ion A in solution
$C_{A,r}$	concentration of ion A in ion-exchange resin
$C_R$	concentration of fixed ionic groups
$C_t$	total exchange capacity
$K$	molar selectivity coefficient
$f_f$	fixed pore ratio
$f_x$	coion exclusion ratio
$f_i$	coion pore ratio
$f_p$	polymer matrix ratio
$f_t$	total pore ratio
$V_0$	bed volume
$V_R$	retention volume
$\epsilon_0$	outer void fraction
$\nu$	average valence number

## REFERENCES

- [1] H. Helfferich, Ion Exchange, McGraw-Hill, New York, 1962, Chap. 5-1.
- [2] F. G. Donnan and E. A. Guggenheim, Z. Phys. Chem., **A162**, 346 (1932).
- [3] F. G. Donnan, Ibid., **A168**, 369 (1934).
- [4] C. Calmon, Reactive Polym., **1**, 3 (1982).
- [5] S. Wakibuchi and K. Yokota, Karyoku Hatsuden, **19**, 1001 (1968).
- [6] K. Kraus and F. Nelson, Proc. Int. Conf. Peaceful Uses At. Energy, Geneva, **7**, 113 (1956).
- [7] E. Hogfeldt (ed.), Stability Constants of Metal-Ion Complexes, Part A, Pergamon, Oxford, 1982.

- [8] K. Takeda, F. Kawakami, and M. Sasaki, Nippon Kagaku Kaishi, **7**, 1138 (1984).
- [9] E. Runter, J. Phys. Chem., **65**, 1027 (1961).
- [10] J. E. Salomon, J. Chem. Soc., p. 2316 (1952).
- [11] S. Takahashi, H. Waki, and S. Ohashi, Proc. 24th Natl. Meet. Chem. Soc. Jpn., Abstr. No. 4113, 858 (1971).
- [12] H. Waki, S. Takahashi, and S. Ohashi, J. Inorg. Nucl. Chem., **35**, 1259 (1973).

Received July 22, 1985